Data-Driven Quantitative Reservoir Characterization and New Insights in Pubei Field of Turpan-Hami Basin, Western China*

Jianbin Ran[1], Haiyin Li[1], Zhengtao Hu[1], Zhe Zhu[1], Jia Chen[1], and Xuejun Wang[1]

Search and Discovery Article #41857 (2016)**
Posted August 29, 2016

*Adapted from oral presentation given at AAPG 2016 Annual Convention and Exhibition, Calgary, Alberta, Canada, June 16-22, 2016

[1]Geophysical Research Institute, BGP Inc. China National Petroleum Corporation, Zhuozhou, Hebei, China (ranjianbin@cnpc.com.cn)

Abstract

Turpan-Hami is a Mesozoic-Cenozoic intermontane basin superimposed on the Cambrian crystalline basement and Paleozoic folded strata in the far northwestern China. This basin has a W-E orientation and is surrounded by the Tian Shan and the Bogda Mountains in the south and north, respectively, and it is about 50,000 km^2 in areal extent. It consists of Turpan Sag to the west and Hami Sag to the east. The sediment fill of the Turpan-Hami Basin contains more than 9 km of continental sediments from Late Permian to Late Tertiary age, in which the Jurassic strata are up to 2.2 km thick and composed of eight 3rd-order sequences. Pubei Field is in the SW part of Turpan-Hami Basin and was discovered in 1993. The Jurassic oil is considered as oil derived from coal and lacustrine mudstone. The reservoir is dominated by alluvial and fluvial and lacustrine sequences of sandstone and siltstone sealed by lacustrine shale. Tectonic, fault geometries, and lithological changes control hydrocarbon traps. Limited amounts of oil and gas were produced from shallow reservoirs in two decades. Exploration challenges were raised from poor quality seismic imaging, caused by gravels with thickness up to 1800 m in the surface as well as harsh environment, and thick coal beds in the subsurface. These resulted in severe seismic wave absorption, whereas the complicated strata by thrusting in Cenozoic time increased the uncertainty of seismic data interpretation. In 2014, seismic low-frequency 3D survey of 304 km^2 was completed by BGP, with a frequency spectrum of 6 octaves, ranging from 1.5 to 96 Hz. The embedded ultra-low-frequency components greatly improve seismic imaging below the coal beds and small faults, as well as lithological changes. A high accurate data-driven quantitative seismic inversion and attribute analysis in sequence stratigraphic framework was achieved by input of high-lateral-fidelity new data. The combined maps of structure, sedimentary facies, and seismic attributes provided the possibilities to conduct quantitative assessment, and the application of spectrum decomposition and reservoir fluid mobility offered an evidence to predict oil and gas within thin reservoirs. Reservoir prediction has been proven by industry oil and gas flow from a new well completed in August 2015. With the improvement of deep seismic imaging, it is possible to conduct seismic evaluation in Paleozoic strata below coal beds in the near future. This case demonstrated that low-frequency seismic technology remains keys to unlocking the oil and gas resources in a mature basin.

Reference Cited

Silin, D.B., V.M. Korneev, G.M. Goloshubin, and T.W. Patzek, 2004, A hydrologic view on Biot's theory of poroelasticity: LBNL Report 54459. Website accessed August 2, 2016, https://publications.lbl.gov/islandora/object/ir%3A122606.

Data-driven Quantitative Reservoir Characterization and New Insights in Pubei Field of Turpan-Hami Basin, Western China

Jianbin Ran, Haiyin Li, Zhengtao Hu, Zhe Zhu, Jia Chen, Xuejun Wang

BGP Inc., China National Petroleum Corporation

June 21, 2016, Calgary, Canada

Outline

- Geology Setting
- Low-frequency Wide Azimuth (LFW) Survey
- Reservoir Characterization
- Conclusions

Presenter’s notes: Presentation includes low-frequency Vibrosis land seismic survey, comparing data quality, imaging and inversion results between conventional 3D and low-frequency 3D data and study of reservoir characterization by low-frequency 3D data in Pubei Field.

Turpan – Hami Basin

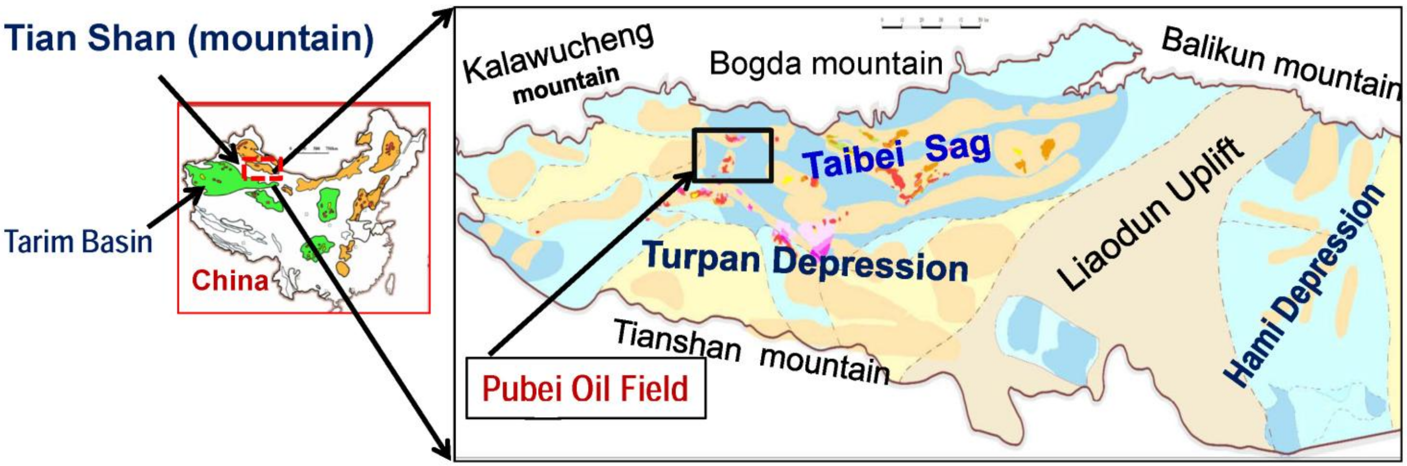

- Mesozoic – Cenozoic intermontane basin in northwestern China
- W-E orientation and surrounded by the Tian Shan in the south and west, and the Bogda Shan in the north
- Consists of Turpan Depression to the west and Hami Depression to the east with total area of 50,000 km^2.

Presenter's notes: Our project area is located in Turpan-Hami Basin, Mesozoic–Cenozoic intermontane basin superposed on the Cambrian crystalline basement and Paleozoic folded strata in far northwestern China, with a W-E orientation and surrounded by the Tian Shan in the south and west and the Bogda Shan in the north. Basin consists of Turpan Depression to the west and Hami Depression to the east, with total area of 50,000 km^2. Turpan Depression descends ultimately to 155 m below sea level, the lowest point in China. It has an extremely arid and hot climate.

Pubei Oil Field

Pubei Oil Field

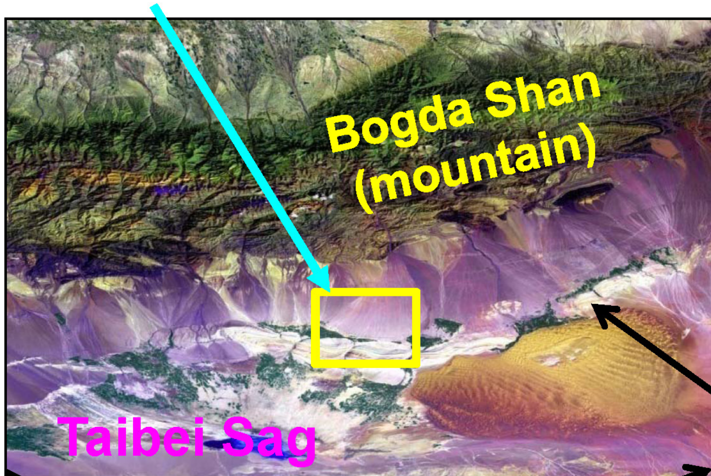

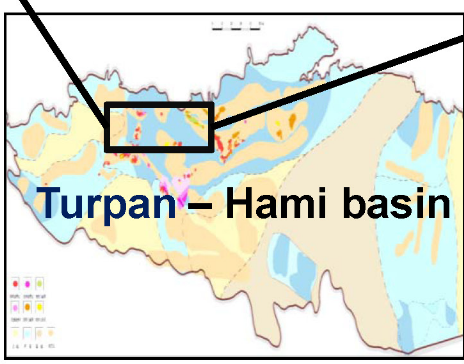

- Located in the northern piedmont belt of the Taibei sag in Turpan depression
- Discovered in 1993
- Limited amounts of oil and gas were produced from the structural or structural-strat traps
- <u>Project objective</u>: to find new structural-strat traps for oil and gas

Huoyan Mountain (98 km long, 9 km wide)

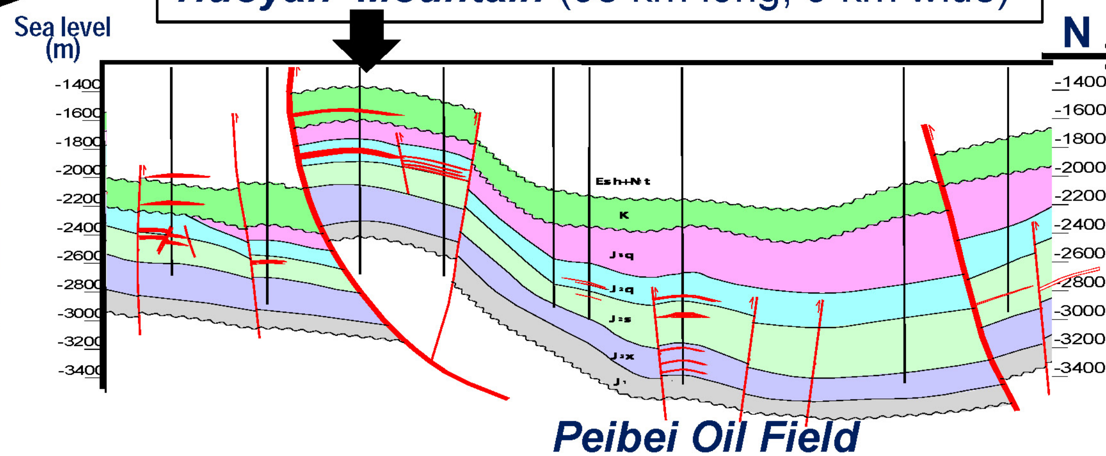

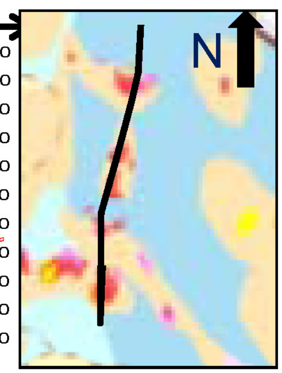

Hydrocarbon profile in Pubei field

Stratigraphy Sequences

★ Case study of reservoir characterization in this presentation

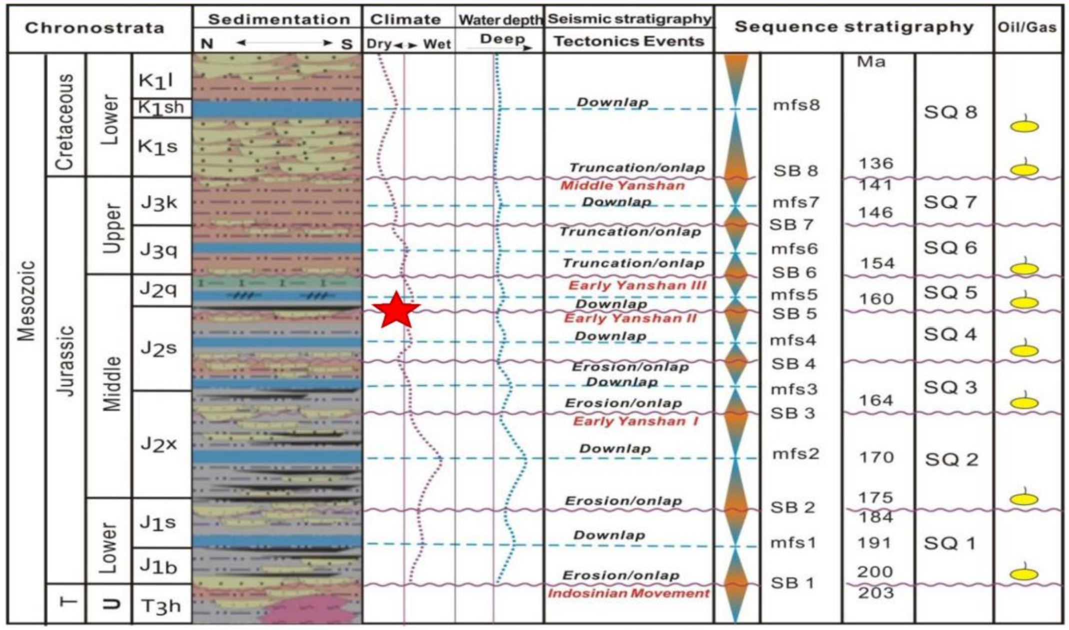

Main reservoir zones

- Eight 3rd–order sequences in the Jurassic and Lower Cretaceous
- Oil and gas discoveries are mainly located in transgressive stages from SQ3 to SQ5
- The reservoir is dominated by sandstone and siltstone of alluvial, fluvial, and lacustrine facies, and sealed by lacustrine shale or coal.
- The main source rocks is the lacustrine mudstone and coal of the Lower Jurassic.

Presenter's notes: Pubei Oil Field's eight 3rd (third)–order sequences are bounded by unconformities or disconformities. The main reservoir zones, in transgressive stages of SQ3 to SQ5, correspond to the Middle Jurassic Qiketai Fm., Shanjianfang Fm., and Xishanyao Fm. Source rocks are Lower Jurassic lacustrine mudstone and coal, as well as those rock types in the Middle Permian and Middle and Upper Triassic. The reservoir zone indicated above by red star has been chosen as the case study of reservoir characterization in this presentation.

Outline

- Geology Setting
- Low-frequency Wide Azimuth (LFW) Survey
- Reservoir Characterization
- Conclusions

Exploration Challenges

◆ **Previous poor data quality caused by:**

- Multi-phases of thick gravels (up to 1800 m) near surface, resulting in serious lateral velocity change and statics problem.
- Multi-coal beds shield the seismic waves.

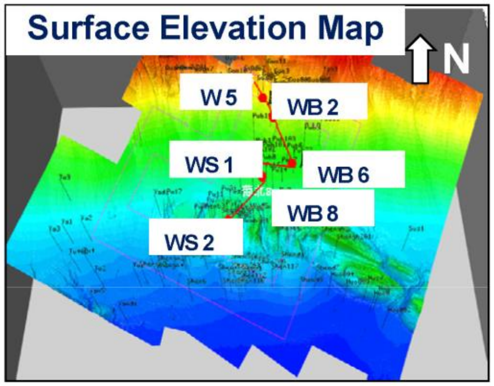

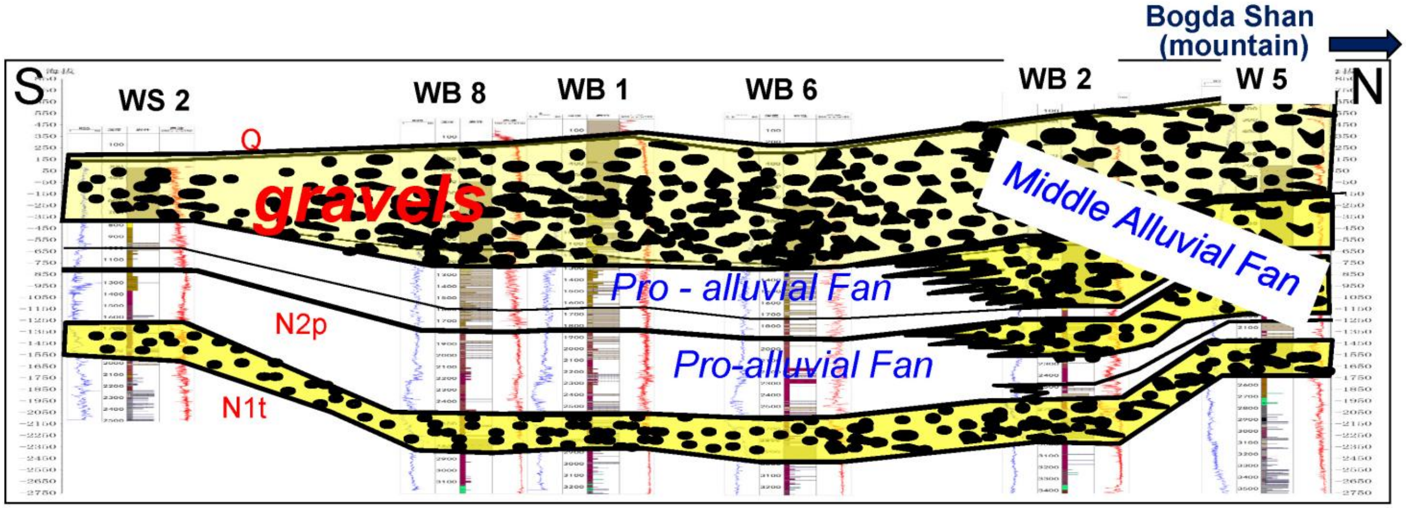

Presenter's notes: The major challenge is related to the thick gravels.

Exploration Challenges

- **Narrow spectrum in conventional 3D data, especially in *low* end, cannot acquire the real geological information**

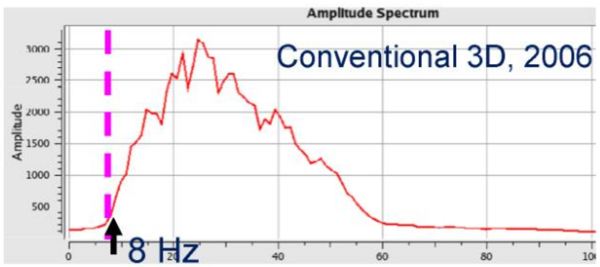

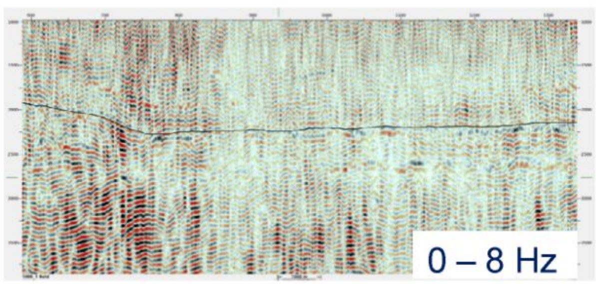

0-8 Hz low-frequency component in conventional 3D missed

- **Low S/N ratio 3D seismic data caused interpretation uncertainty**

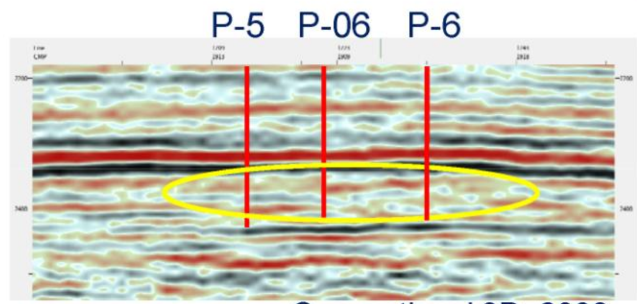

Conventional 3D, 2006

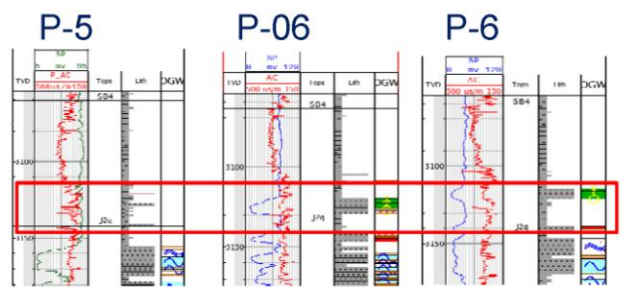

Lithology changes identified, by drilling data, between wells P-5 & P-06

Presenter's notes: The second challenge is from the narrow spectrum in conventional 3D data, especially in *low* end. The conventional 3D data was collected in 2006; the seismic information between 0 and 8 Hz was almost missed. The third challenge is from the low-signal-to-noise-ratio 3D data. From the three wells, the data show sandbody changes. However, these types of changes cannot be recognized in this conventional 3D seismic section.

Low-frequency Wide Azimuth (LFW) Survey

New 3D survey acquired in 2014

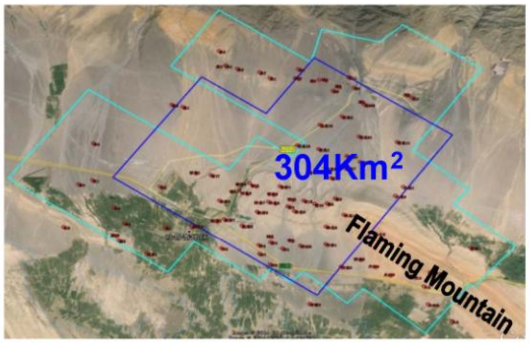

Merge reprocessing 3D, 2006 - 2013

Low-frequency 3D, 2014

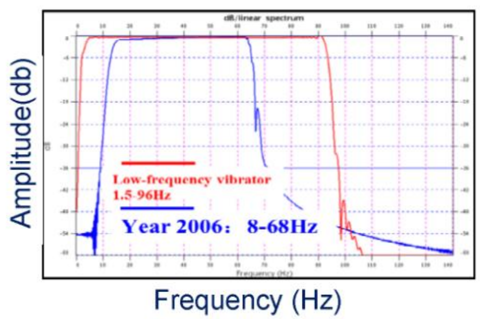

Conventional 3D, 2006	low-frequency 3D, 2014
Bandwidth: 8 - 68	Bandwidth: 1.5 - 96
Bin size: 20 X 20	Bin size: 20 X 20
Fold: 72	Fold: 768
Aspect ratio: 0.25	Aspect ratio: 0.75

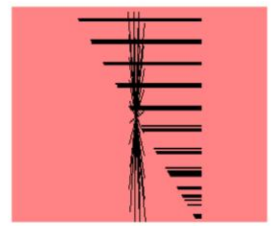

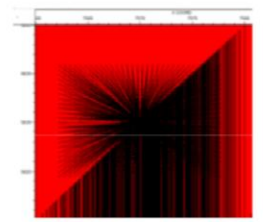

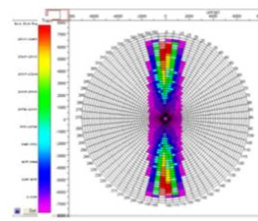

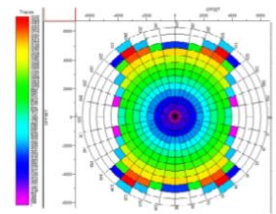

Comparison of conventional and low-frequency Vibroseis survey

Presenter's notes: In 2014, BGP conducted, in an area of 304 square km, low-frequency Vibroseis land survey. It was the first low-frequency Vibroseis land survey in Turpan-Hami Basin. The bandwidth of conventional 3D in 2006 was 8 to 68 Hz, the fold was 72. The low-frequency Vibroseis had bandwidth of 1.5 to 96 Hz; the fold was 768; the aspect ratio increased from 0.25 to 0.75. This means the bandwidth of low-frequency Vibroseis 3D (red line) is much wider than that of the conventional 3D (blue line); it allowed us to record unaliased signal and noise and to do a much better job with noise attenuation during processing.

Low-frequency Wide Azimuth (LFW) Survey

Main processing

Tomographic statics

↓

Well constrained

↓

OVT

↓

Anisotropic prestack depth migration

QC ←

QC steps by Interpretation

Well controlled surface consistent deconvolution

Prestack time migration velocity analysis

CRP gather protection monitoring

Azimuth Gather

PSDM horizon model

PSDM Layer velocity model

PSDM Well seismic error analysis

Low-frequency Wide Azimuth (LFW) Survey

BGP KZ28LFV3 Vibrator: extended octave from 3 to 6

Low-frequency Vibroseis, 2014

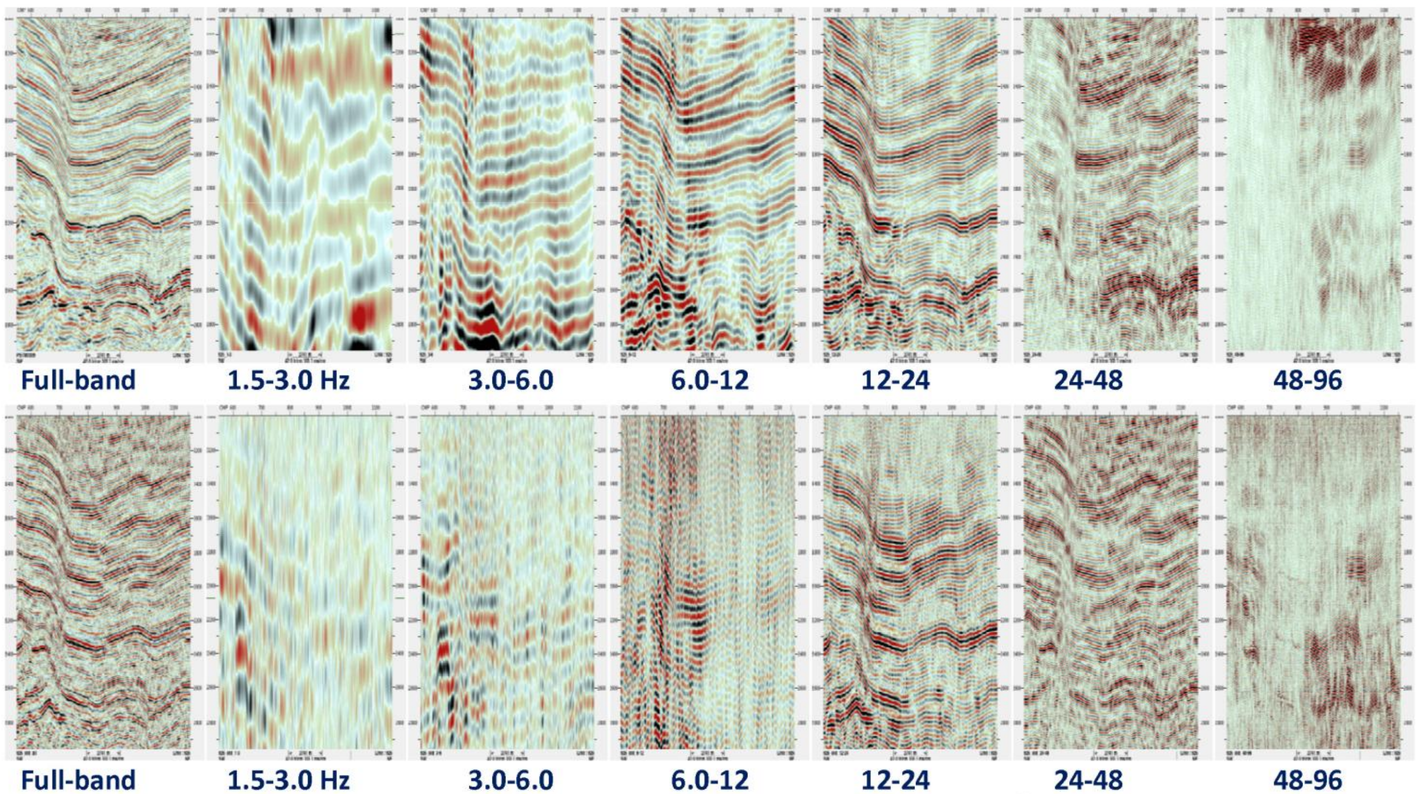

Conventional 3D, 2006

Presenter’s notes: Amplitude spectrum differences between low-frequency and conventional 3D:
At 1.5-3 Hz, as well as 3.0-6 HZ, distinguishable information is seen in low-frequency Vibroseis data, whereas it is unclear in conventional 3D.

Low-frequency Wide Azimuth (LFW) Survey

Better imaging below thick coal-beds

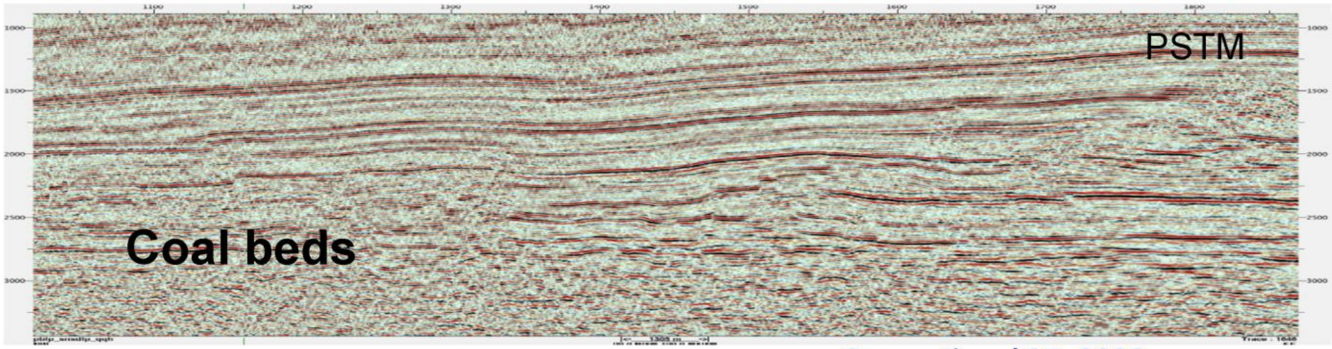

Conventional 3D, 2006

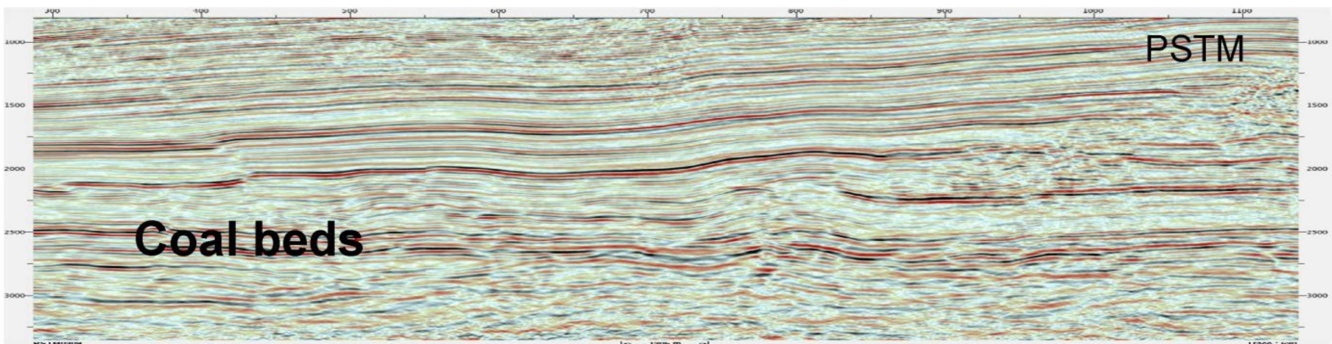

Low-frequency Vibroseis, 2014

Improved seismic imaging in deep zones

Presenter's notes: Upper part is conventional 3D data collected in 2006—due to absorption from Jurassic coal beds and narrow spectrum, the imaging is unclear. Lower part is the low-frequency Vibroseis data acquired in 2014. Exploration targets on conventional 3D data were focused on the shallow part above coal seam. Now, we can use low-frequency Vibroseis data to conduct research on both shallow and deep strata.

Low-frequency Wide Azimuth (LFW) Survey

High S/N ratio and better imaging for fault identification

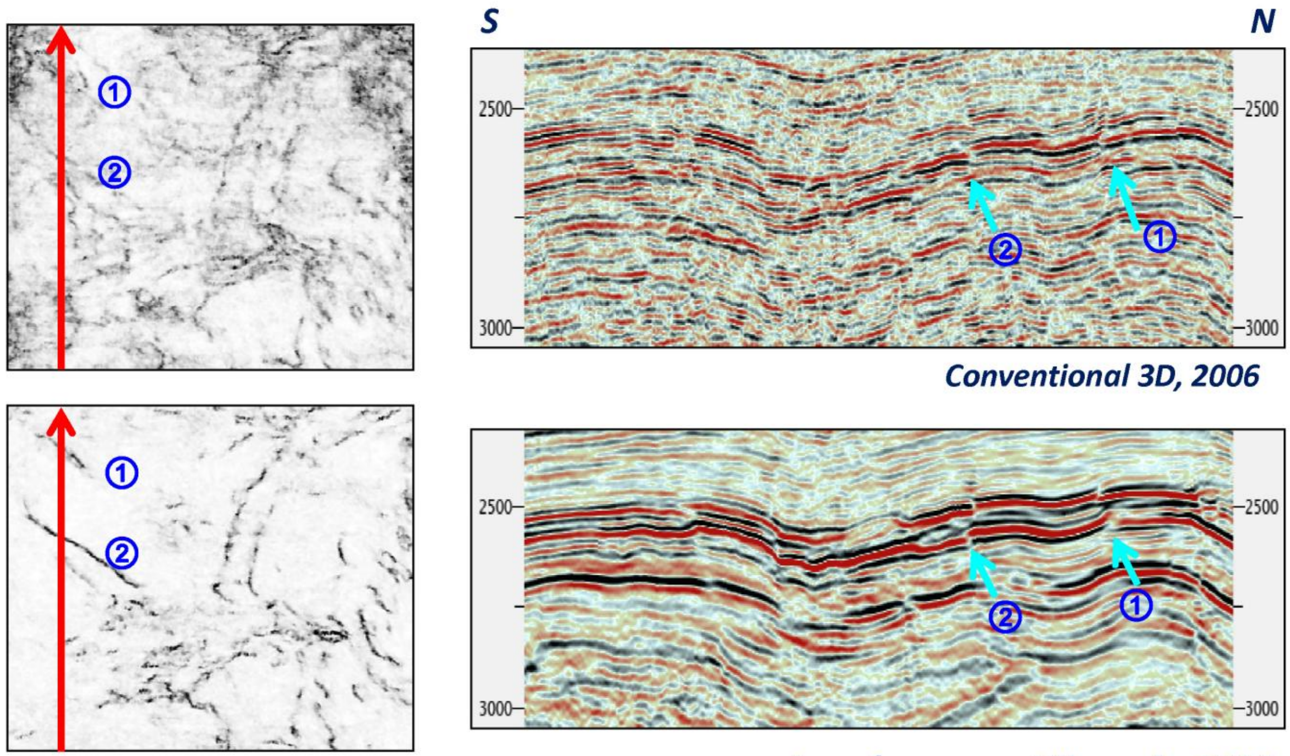

Conventional 3D, 2006

Low-frequency Vibroseis, 2014

Coherence

Presenter’s notes: The upper part is from conventional data and the lower is low-frequency data. The minor faults are presented on both coherence slice and seismic profile in low-frequency data. Resolution has an obvious improvement in the low-frequency data.

Low-frequency Wide Azimuth (LFW) Survey

Broaden bandwidth Improved lateral fidelity for seismic inversion

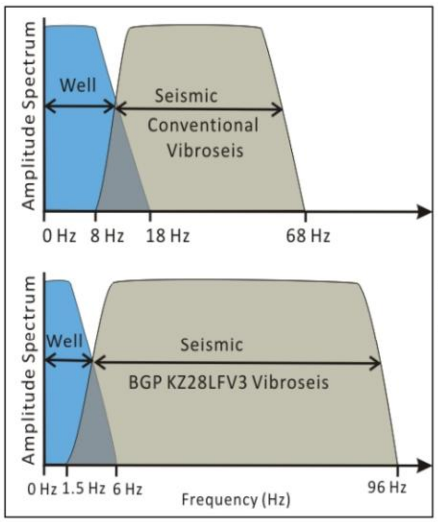

Schematic relationship of seismic bandwidth and well low-frequency model used in seismic inversion

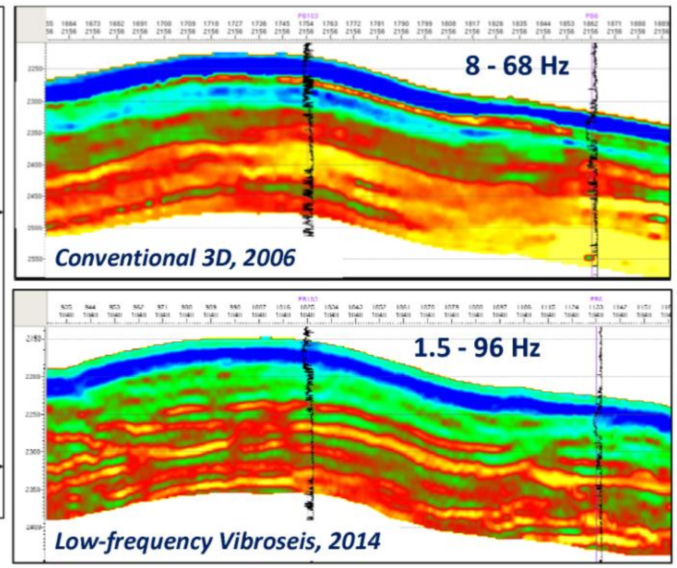

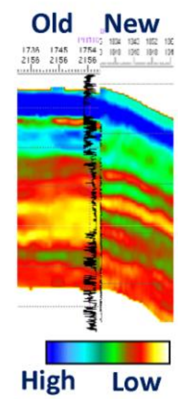

More accurate inversion resulted with high lateral and vertical fidelity by low- frequency Vibroseis data

Presenter's notes: Another important utilization of low-frequency components is in the seismic data inversion. Left image shows the different spectrum used during seismic inversion. During the inversion by conventional 3D data, only 8-68 Hz seismic data can be used for data inversion; the spectrum from 0 to18 Hz is borrowed from well logs, whereas with low-frequency Vibriseis data, the spectrum from 1.5 to 96 Hz can be directly used. Only the small parts of the spectrum between 0 and 6Hz are borrowed from well data. Thus, low-frequency Vibriseis data can provide higher fidelity data for seismic inversion. The upper part is impedance inversion from conventional 3D seismic data, and the lower part is from the low-frequency data. Resolution of the low-frequency data is much higher than that from conventional 3D data.

Low-frequency Wide Azimuth (LFW) Survey

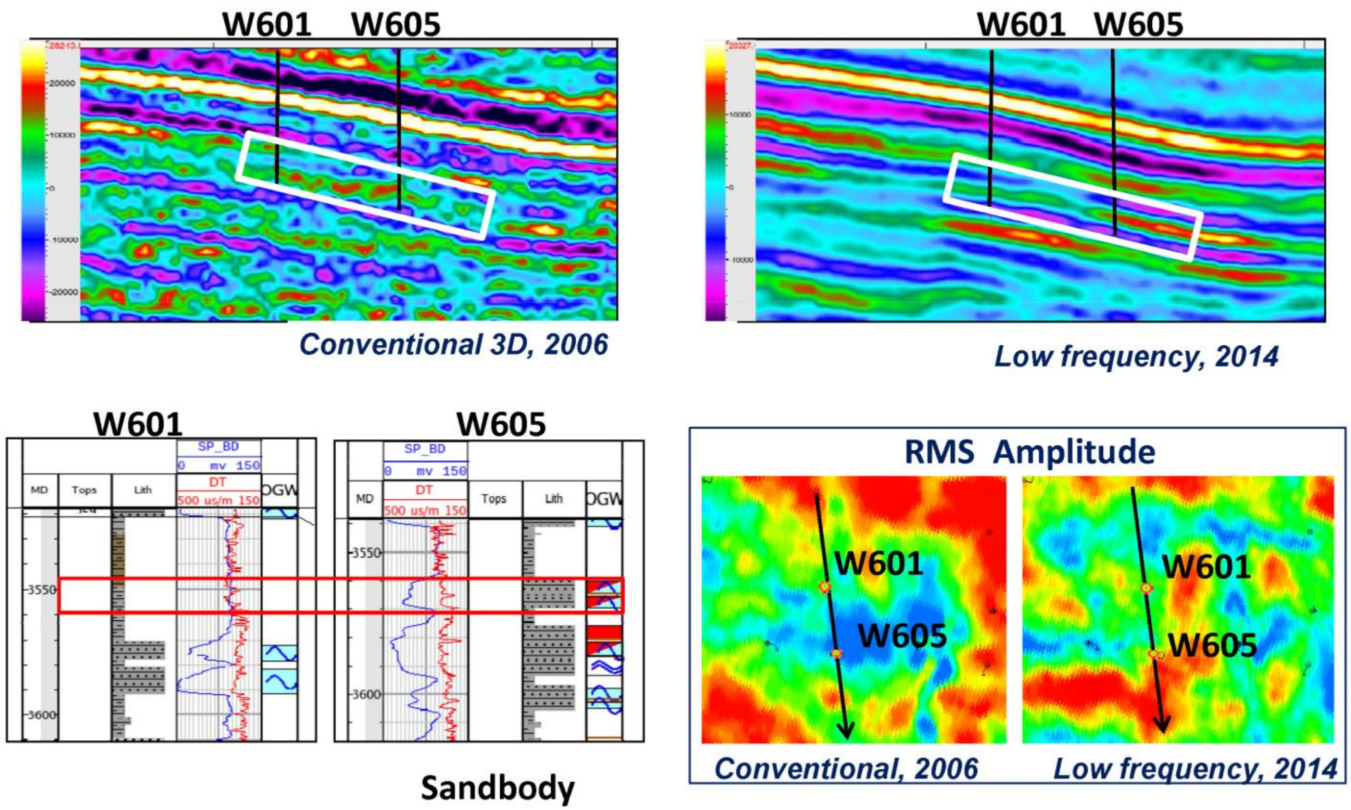

Inversion result better match with well information

Presenter's notes: Seismic attributes of lithologies of low-frequency data are more consistent with drilling results than by using conventional 3D. Note also the differences in RMS amplitude between the two types of seismic.

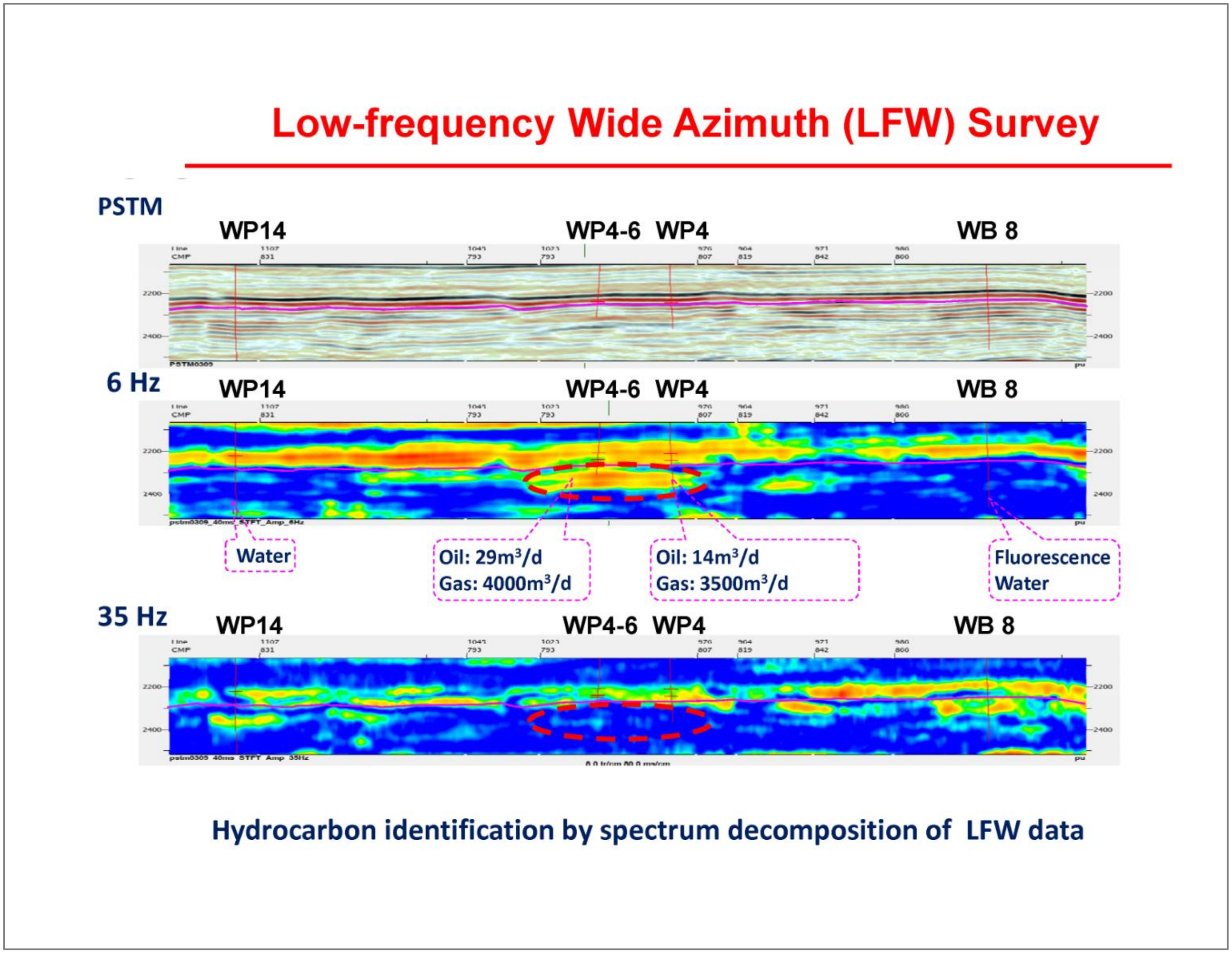

Presenter's notes: This slide presents the cross sections through four wells, the upper is the seismic PSTM section; the middle is 6 Hz, and the lower is 35 Hz common frequency profile. Oil and gas have been found in well WP4-6 and WP4, whereas WP14 and WB8 were dry wells. Higher energy amplitude appears in 6 Hz common frequency profile below the oil-bearing well WP4-6 and WP4; it does not show beneath dry wells WP14 and WB8. This feature results from the attenuation of fluid-saturated reservoir to high-frequency components of seismic waves, called low-frequency shadow.

As for 35 Hz common frequency profile in the same areas, we can't see these features.

Low-frequency Wide Azimuth (LFW) Survey

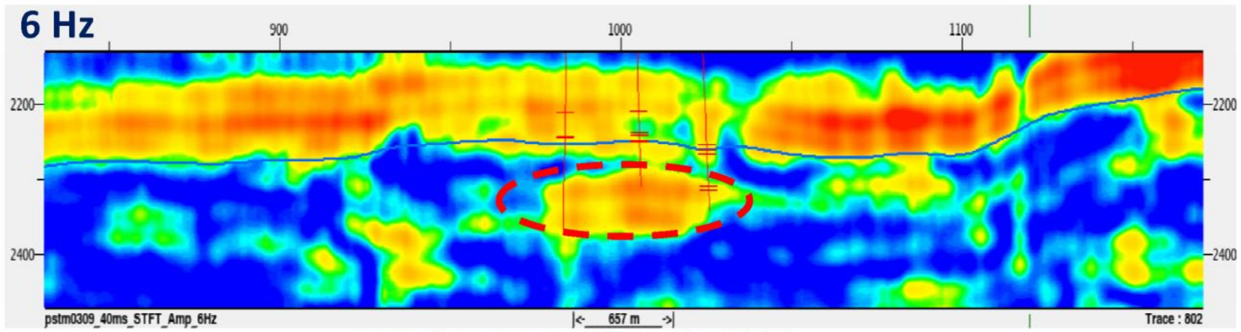

Low-frequency Vibroseis, 2014

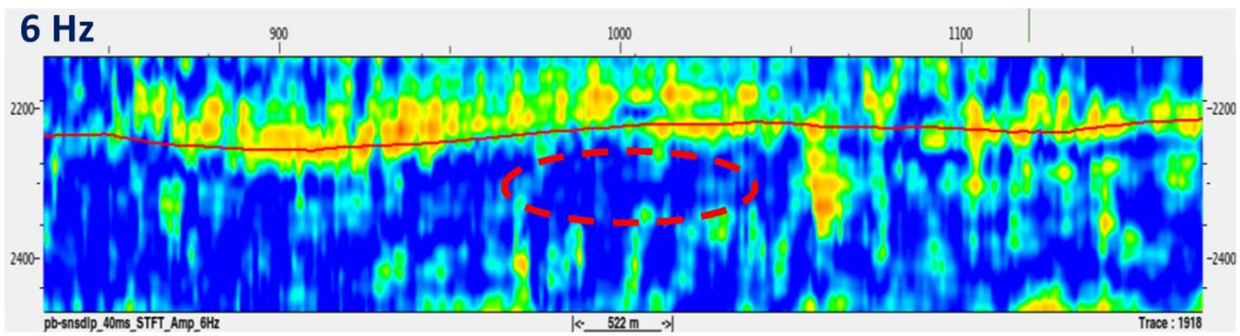

Conventional 3D, 2006

Hydrocarbon identification by spectrum decomposition of LFW data

Presenter's notes: Both sections are 6 Hz common frequency profiles. The higher energy amplitude; that is, the low-frequency shadow appears in fluid-saturated reservoir in low-frequency data; this feature is not visible in the conventional 3D.

Outline

- Geology Setting
- Low-frequency Wide Azimuth (LFW) Survey
- Reservoir Characterization
- Conclusions

Reservoir Characterization in lower part of SQ5

Workflow

detailed horizon calibration

Minor-fault identification

Variable velocity modeling and mapping

Sandbody interpretation within sequence stratigraphy framework

inversion

DHI by spectrum decomposition
and fluid mobility analysis

Integrated evaluation of structural - strat traps

Detailed horizon calibration

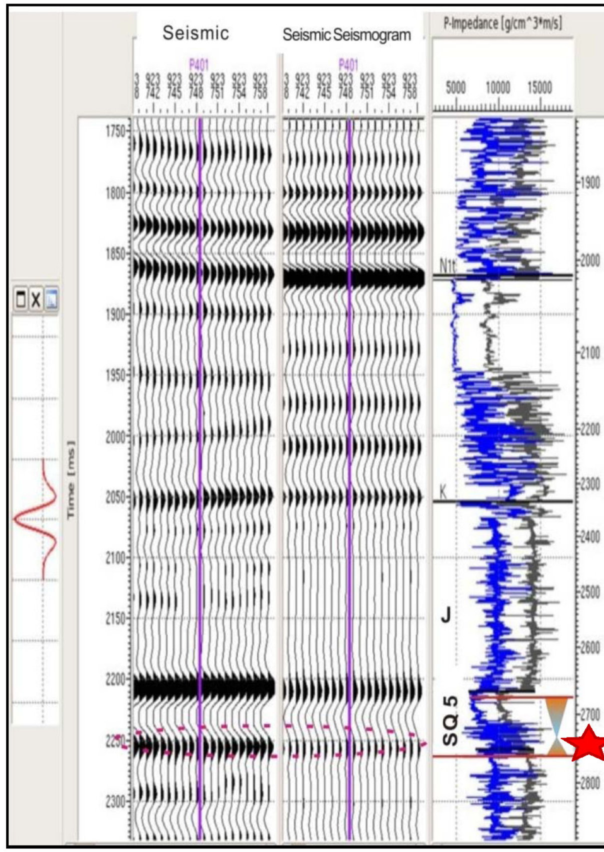

Outcrop

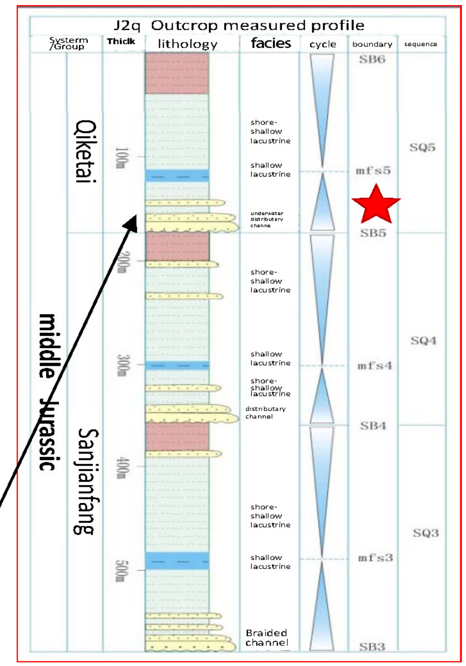

pay zone in lower part of SQ5

Minor-fault identification

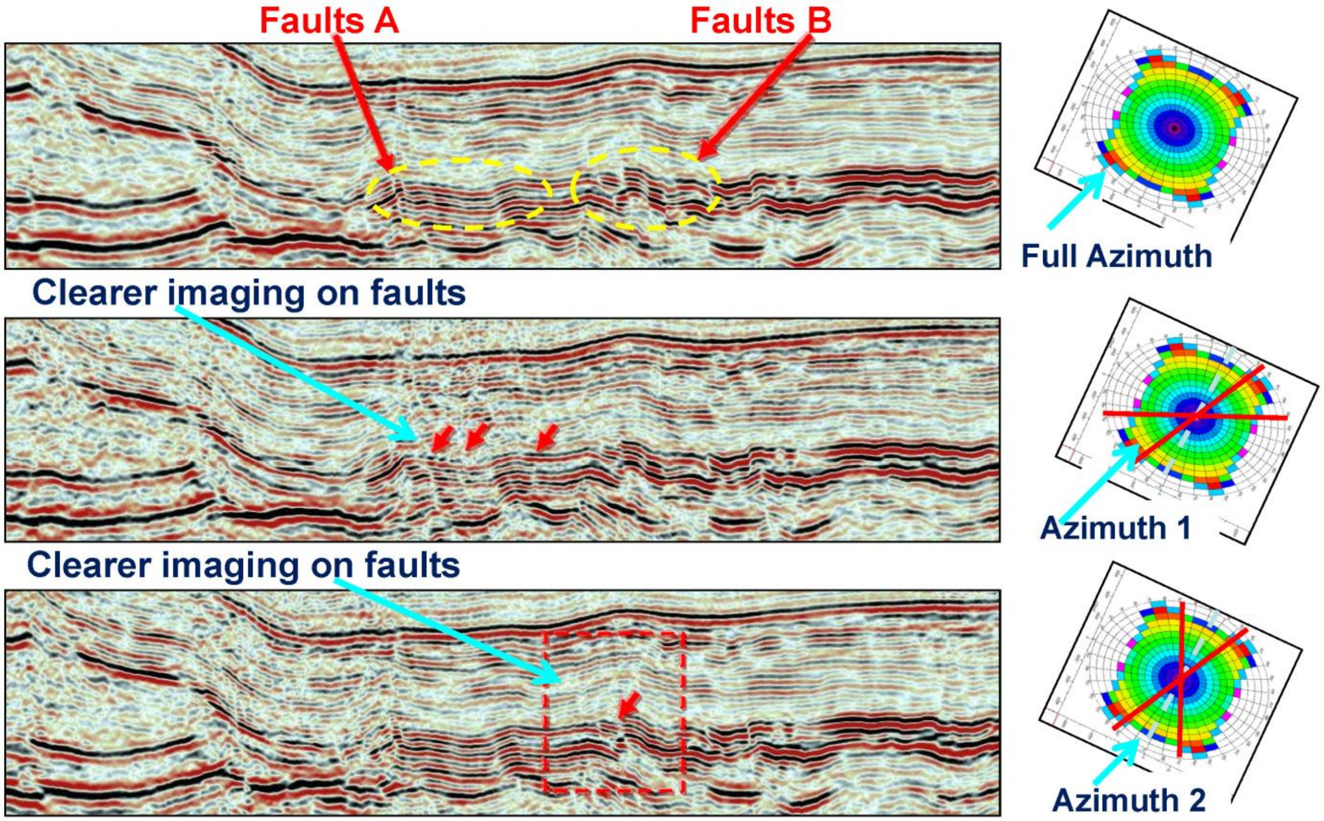

Easy minor-fault identification with OVT (Offset Vector Tile) data

Presenter's notes: OVT data was used to identify small faults. Upper section corresponds to full azimuth; imaging of faults A are clearer in middle section, corresponding to azimuth 1; whereas, the faults B are clearer in lower section, corresponding to azimuth 2. Different faults can be better imaged by different azimuths.

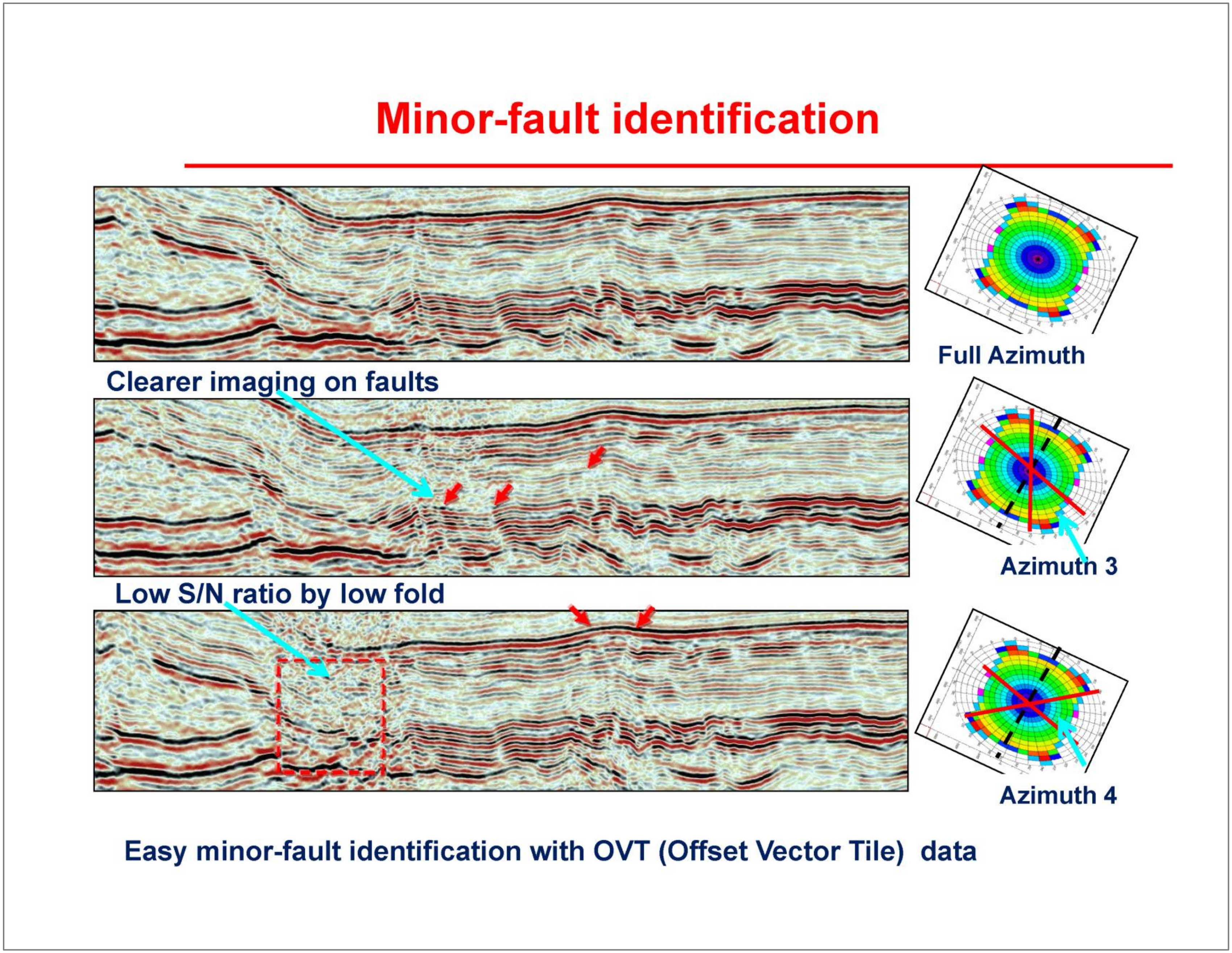

Presenter's notes: The faults are better imaged corresponding to azimuth 3. With the low fold in azimuth 4, the imaging in red rectangle area presents a low-signal-to-noise ratio.

Minor-fault identification

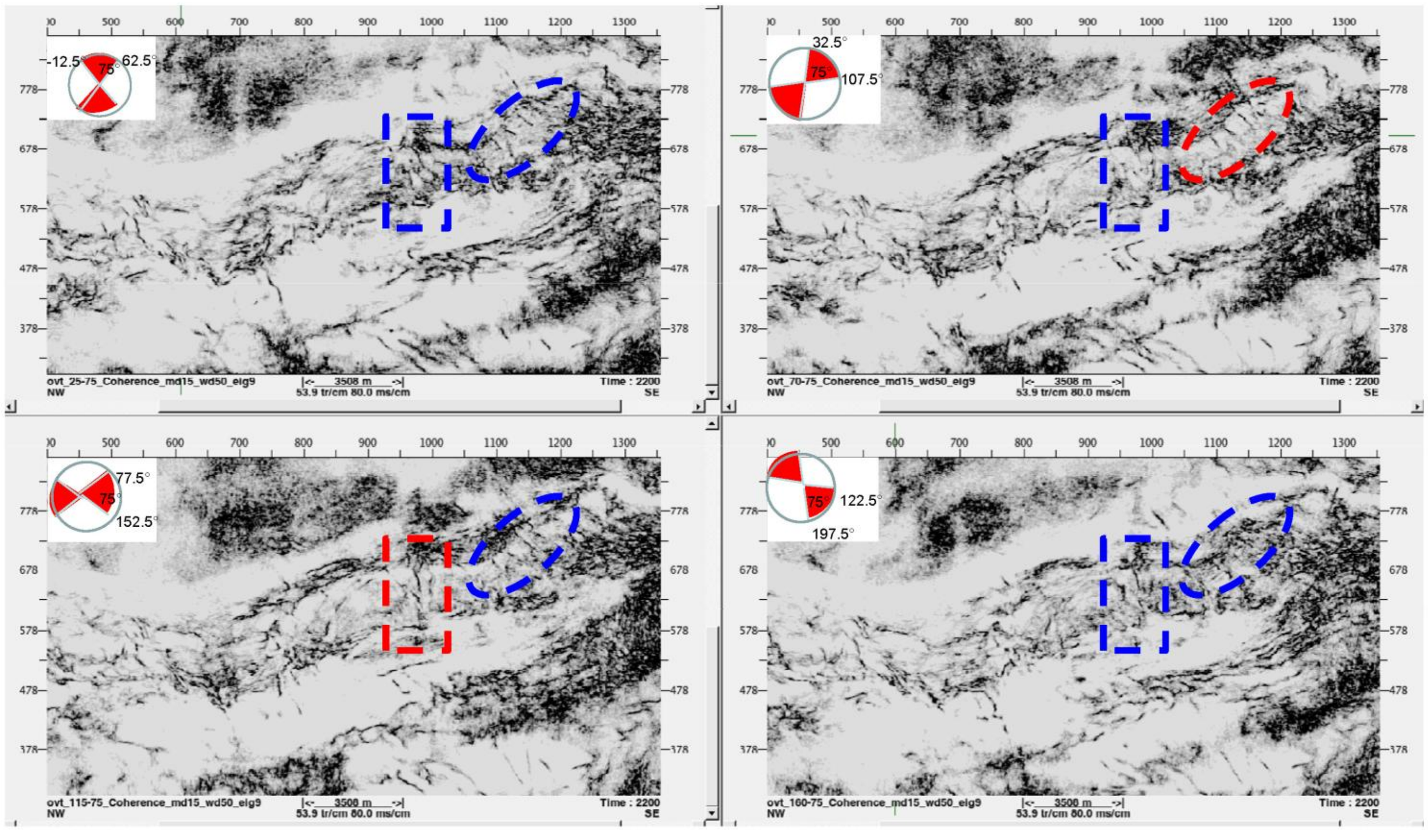

Clearer imaging on faults in the direction perpendicular to faults

Presenter's notes: These four coherence slices correspond to four different azimuths. Better imaging on faults is achieved when the azimuth is in the direction perpendicular to fault.

Minor-fault identification

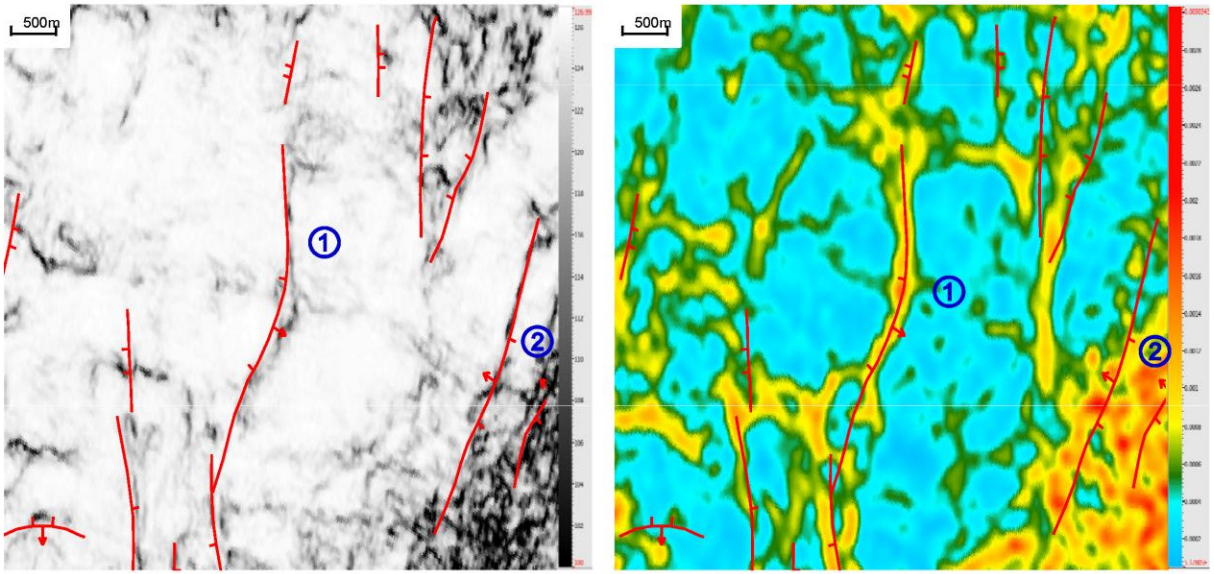

Coherence Curvature

Different attributes used for fault interpretation

Presenter’s notes: Attribute analysis of low-frequency data makes a realistic interpretation of fault geometry. Based on the coherence and curvature maps, we have described the areal configurations of the faults.

Sandbody interpretation within sequence stratigraphic framework

Sedimentation facies of SQ5

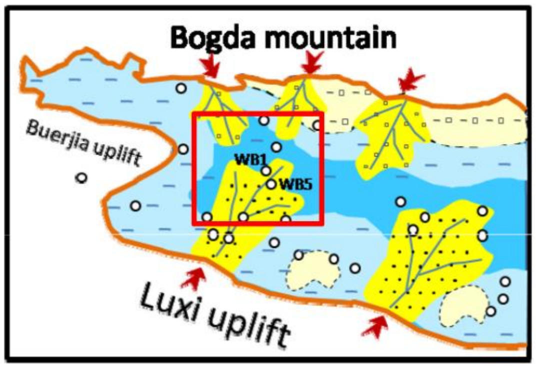

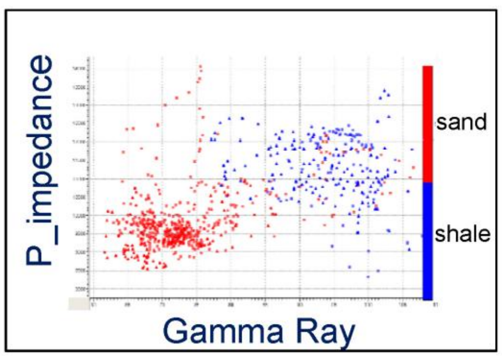

Cross plot of well information

- Regional sedimentary facies distribution of sequence stratigraphic study provide a basic geometry of sandbodies distribution
- P_Impedance (PI) inversion characterize sandstone distribution

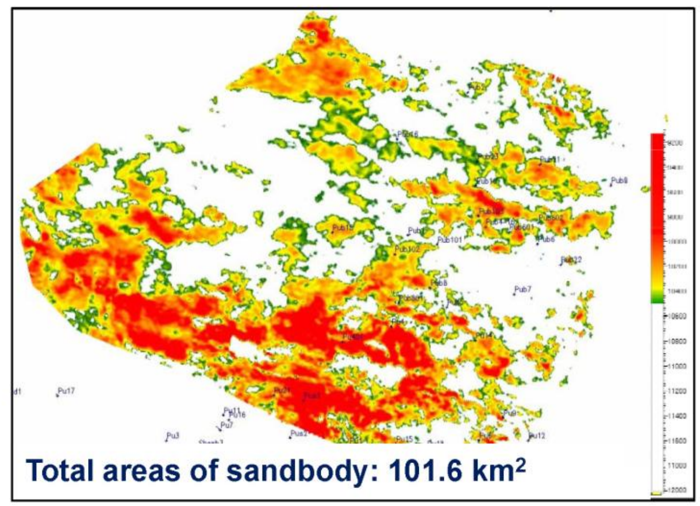

Sandbody distribution in the lower part of SQ5
(P_impedance < 105000)

Presenter's notes: Regional sedimentary facies distribution from sequence stratigraphic study provided a basic geometry of sandbody distribution. From cross plot of P_impendence and Gamma Ray , lower impendence corresponds to sand, whereas higher impendence corresponds to shale.

Reservoir prediction by inverted porosity maps

Cross plot of P_impedance & porosity

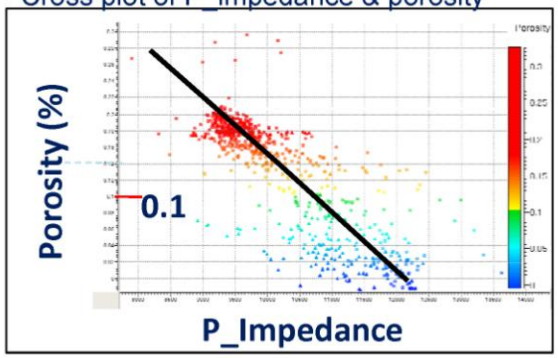

Porosity cutoff: 10%

Porosity in Lower part of SQ5

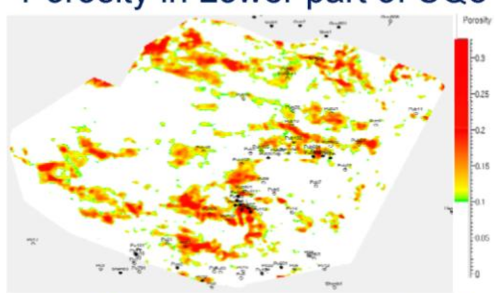

Cutoff: 10% Area:43.2km^2

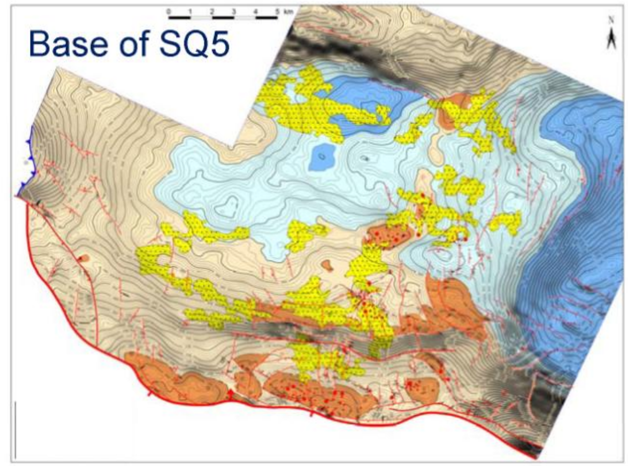

- **Structural-strat traps/areas: 16 /43.2 km^2**

sweet areas of structural-strat trap can be identified by combination of structural map and porosity map

Presenter's notes: One goal of this study is to quantify the porosity of the reservoir from seismically-derived elastic parameters. From the cross plot of P-wave impedance and porosity in well WB10, there is a linear relationship between them. In upper left, 0.1 is chosen as porosity of 10% as a cutoff. In lower left, map is the inverted porosity from P_impedance at the base of SQ5. Based on cutoff of 10%, prospect areas are 43.2 sq. km, with 16 structural-strat traps, some of which have been drilled and confirmed.

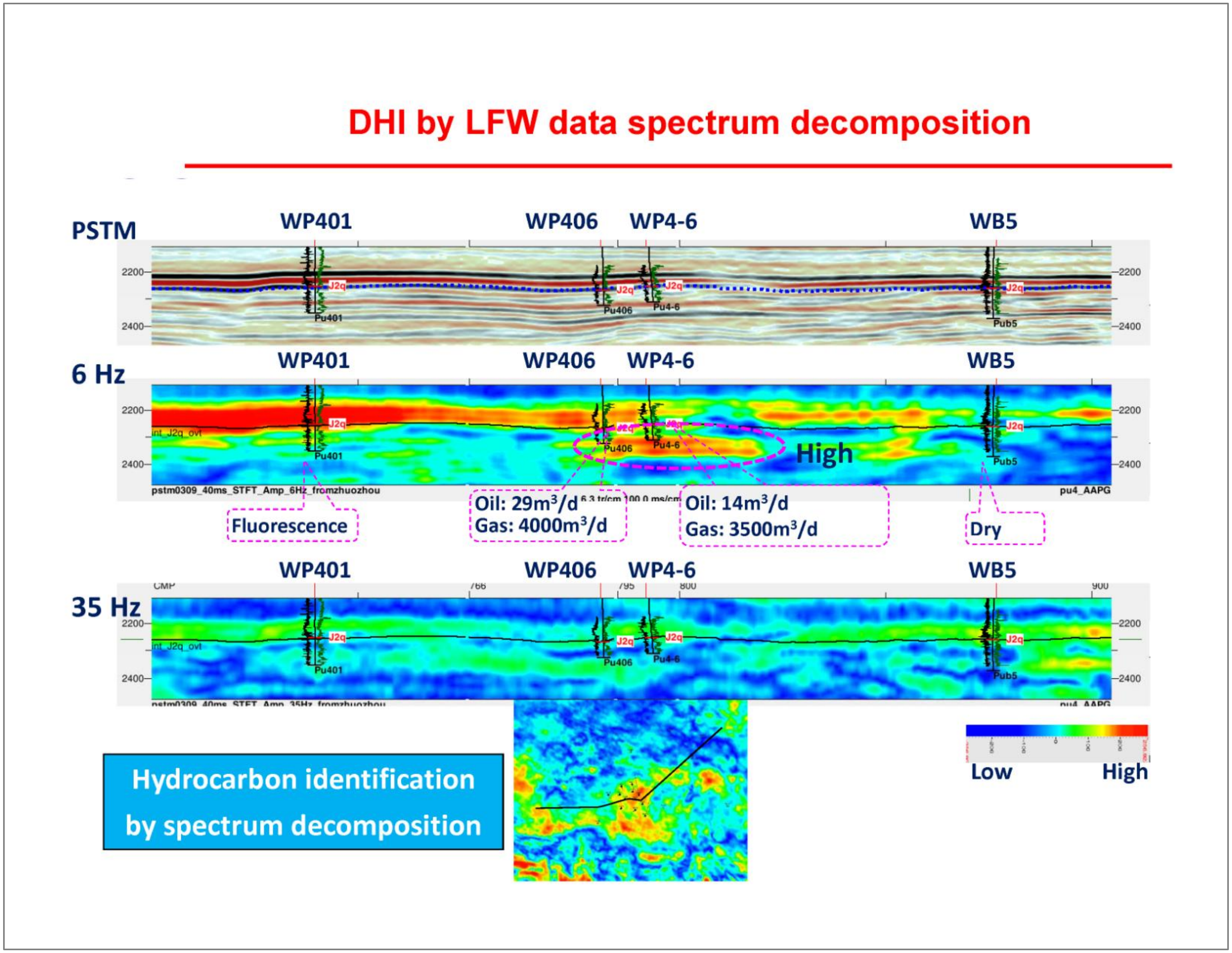

Presenter's notes: In recent years, attributes based on spectrum decomposition, such as low- frequency shadow with hydrocarbon and fluid mobility, have provided new approaches for reservoir prediction and fluid identification. This slide illustrates low-frequency shadow. It presents the comparison of time-frequency analysis of 6 Hz and 35Hz common frequency profiles through 4 different wells. Higher energy amplitude appears in 6 Hz common frequency profile below the oil-bearing well WP406 and Wp4-6; it is not shown in 35 Hz common frequency profile in same areas. In the dry wells, these features are not visible.

DHI by LFW data spectrum decomposition

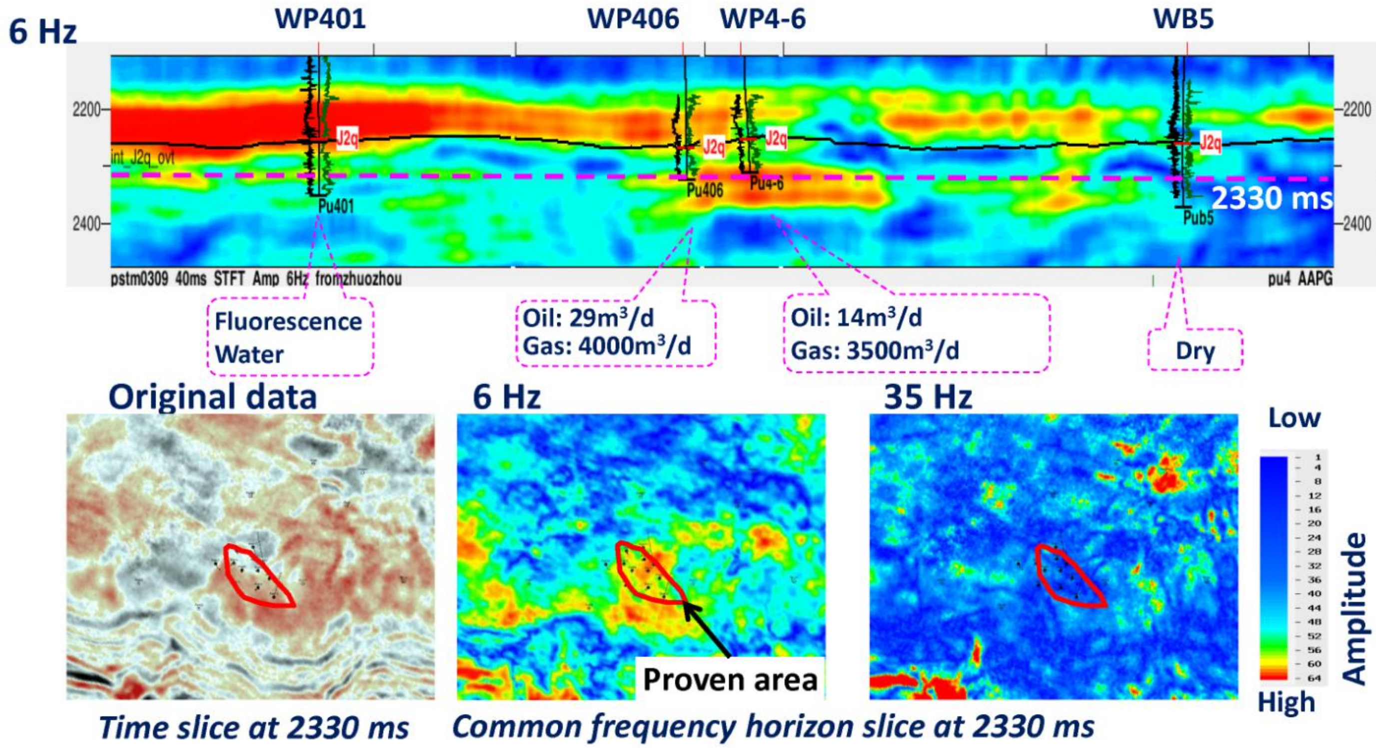

DHI by spectrum decomposition

Presenter's notes: Regionally, these kinds of different amplitude features can be seen in 6 Hz and 35 Hz common frequency time slices. Higher energy amplitude appears in 6 Hz common frequency time slice and relatively low amplitude in 35 Hz common frequency time slice. Red polygon is reserve-proven area; now, we pay more attention to higher energy amplitude area outside it. Because typical low-frequency shadow cannot always be seen, we need some other methods of fluid identification to help us identify the oil-gas potential of the trap. Fluid mobility is another very effective method .

DHI by LFW data spectrum decomposition

Reservoir fluid mobility can be good evidence for prediction of oil and gas within thin reservoirs

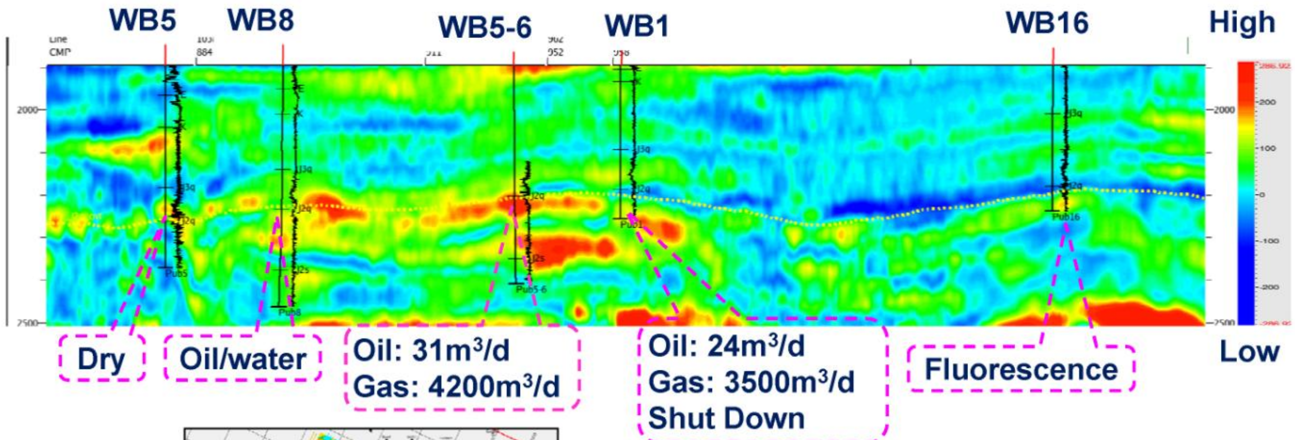

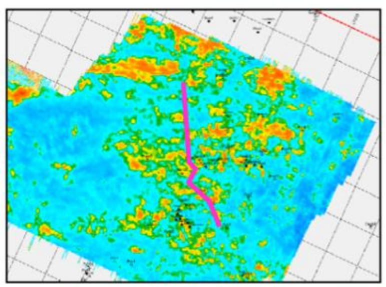

Slice of reservoir fluid mobility

Fluid mobility M is expressed as follows:

$$M \approx F\left(\frac{\rho}{\mu}\right)K \approx \left(\frac{\partial R}{\partial f}\right)^2 f$$

F: fluid function	K : permeability
P: fluid density	*R: amplitude*
μ: fluid viscosity	*f: signal frequency*

(Silin et al. 2004)

Presenter's notes: Here fluid mobility is shown. Typical low-frequency shadow cannot always be seen; methods of fluid identification can help identify the oil-gas potential of the trap. Fluid mobility is a function of fluid function, fluid density, viscosity, permeability, seismic wave amplitude, and signal frequency. Fluid mobility reflects the permeability and fluid properties within the reservoir; so it can be used to predict best quality of reservoir. Upper picture is a cross section through 5 wells, based on the drilling data; we can see that the oil-gas-bearing zones have the features of 'low-frequency and strong-amplitude'; that is, the higher amplitude (red) corresponds to the higher value of reservoir fluid mobility. Based on the slice of reservoir fluid mobility, we can estimate the regional distribution of oil and gas. This map can help us make good well planning.

Proposed Well in the potential areas and drilling results

Drilling results of WB406 (new well)

WB 406

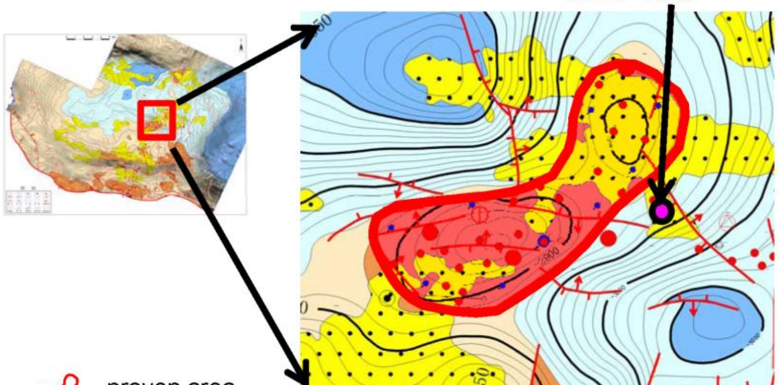

proven area

WB 406

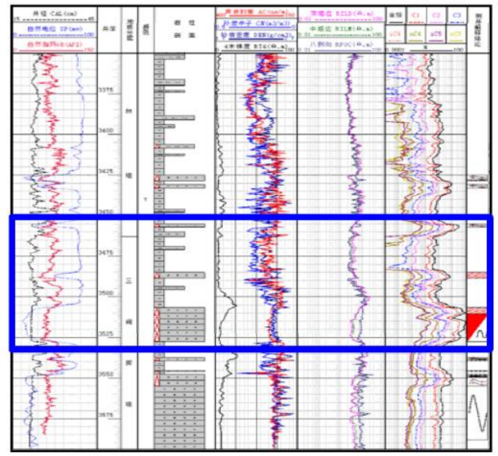

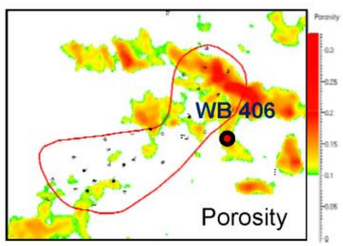

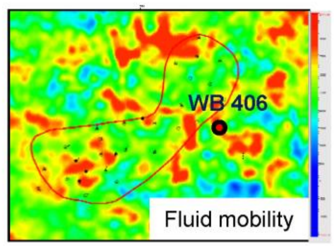

WB406 by well logging

oil: 7.6m/2 units

Oil/water: 17m/1 unit

Oil production: $9m^3$/day。

Combination of structural–strat trap map, porosity map and DHIs provided best reservoir areas for drilling plan

Presenter's notes: Based on the structural-strat trap map, porosity map and DHIs maps, we designed an assessment well, WB406, outside of proven area, drilled in May 2015 . Oil has been found, and production is $9m^3$/day. Drilling results show that the predicted reservoir parameters are reliable.

Proposed Well in the potential areas and drilling results

Drilling results of WB801 (new well)

WB 801

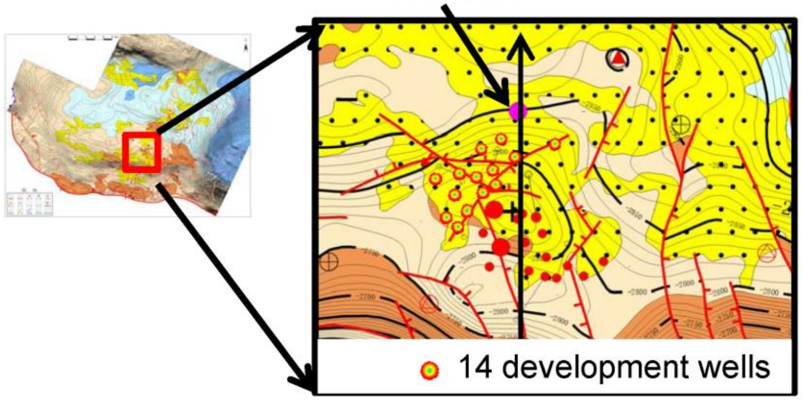

WB 801

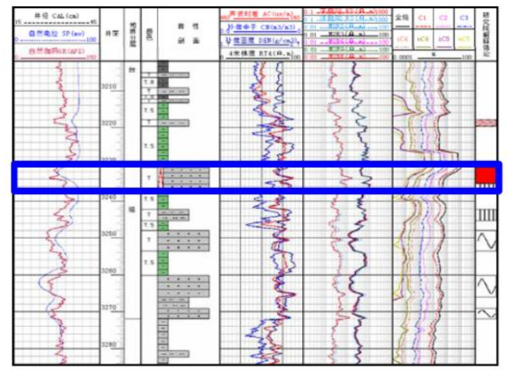

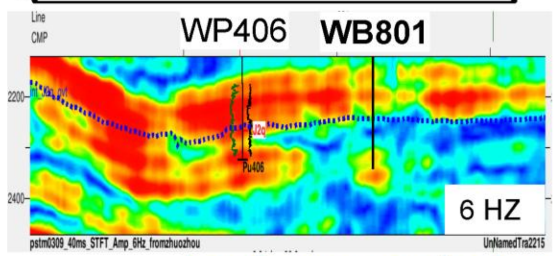

low-frequency shadow

WB801 by well logging

oil: 4.4m/1 unit

Poor oil: 1.8m/1 unit

Oil/water: 4.8m/1 unit

Oil production: 5m^3/day。

Combination of structural–strat trap map, porosity map and DHIs provided best reservoir areas for drilling plan

Presenter's notes: WB 801 was a delineation well outside Pubei Oil Field, drilled last August. Drilling results are consistent with predictions of the reservoir parameters. Oil has been found; production is 5m3/day. After the success of this well, we proposed 14 development wells in this area. All these wells obtained commercial oil flow. By the end of May 2016 , about 43,000 tons (~300,000 bbls) of oil have been produced.

Well proposals for the next phase of drilling

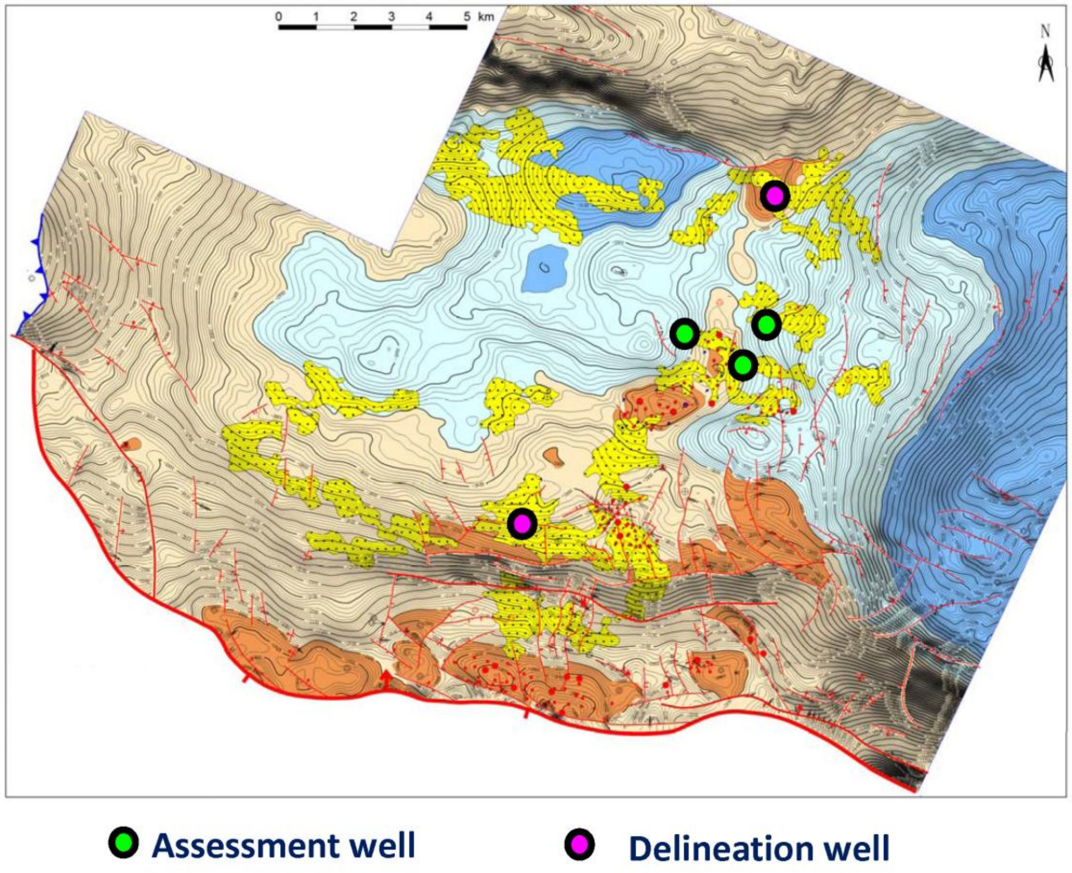

Presenter’s notes: We shall drill more wells in these structural-strat traps in the near future. We think BGP low-frequency Vibroseis land survey technology is making and will make great contribution to petroleum industry growth globally.

Outline

- Geology Setting
- Low-frequency Wide Azimuth (LFW) Survey
- Reservoir Characterization
- Conclusions

Conclusions

- BGP KZ28LFV3 Vibrator and Vibroseis can provide 1.5 Hz low-frequency broadband seismic data.

- LFW technology delivers a high S/N ratio, high fidelity, broadband seismic data for minor-fault identification, enabling better penetration beneath coal-beds.

- As for mature field, the integrated study of structure, sedimentary facies in sequence stratigraphic framework and seismic attributes provide the possibilities for conducting quantitative assessment. Low-frequency contents provide a clearer stratigraphic interpretation of high heterogeneous sandbodies.

Thanks!

Welcome to China, welcome to BGP